

This item is the archived peer-reviewed author-version of:

Microbeam X-ray fluorescence and X-ray absorption spectroscopic analysis of Chinese blue-and-white kraak porcelain dating from the Ming dynasty

Reference:

De Pauw E., Tack P., Verhaeven E., Bauters S., Acke Lien, Vekemans Bart, Vincze Laszlo.- Microbeam X-ray fluorescence and X-ray absorption spectroscopic analysis of Chinese blue-and-white kraak porcelain dating from the Ming dynasty
Spectrochimica acta: part B: atomic spectroscopy - ISSN 0584-8547 - 149(2018), p. 190-196
Full text (Publisher's DOI): <https://doi.org/10.1016/J.SAB.2018.08.006>
To cite this reference: <https://hdl.handle.net/10067/1529680151162165141>

Microbeam X-ray fluorescence and X-ray absorption spectroscopic analysis of Chinese blue-and-white kraak porcelain dating from the Ming dynasty

E. De Pauw^{a*}, P. Tack^a, E. Verhaeven^a, S. Bauters^{a,b}, L. Acke^c, B. Vekemans^a, L. Vincze^a

^aX-ray Microspectroscopy and Imaging group, Department of Chemistry, Ghent University, Krijgslaan 281, B-9000 Gent, Belgium

^bDUBBLE, European Synchrotron Radiation Facility (ESRF), 71 Avenue des Martyrs, 38000 Grenoble, France

^cConservation and Restoration, Antwerp University, Blindestraat 9, 2000 Antwerp, Belgium

*Corresponding author: ella.depauw@ugent.be

Abstract

Microbeam X-ray fluorescence (XRF) spectroscopy is applied, next to an art-historical analysis, to determine the time and place of origin of Chinese blue-and-white porcelain. In the performed experiments, two groups of kraak porcelain samples (A and B) have been analyzed with XRF spectroscopy to obtain quantitative data, (trace) elemental distributions and fingerprints within different regions of interest. The outcome was processed with Principal Component Analysis (PCA), and with the obtained results it was possible to conclude that the two groups show similar elemental fingerprints and were manufactured in the same time period with a comparable use of raw materials. Additionally, X-ray absorption spectroscopy (XAS) measurements have been performed on the pigment layer, confirming the use of Cobalt Blue as an underglaze pigment.

Keywords: X-ray Fluorescence spectroscopy, X-ray Absorption spectroscopy, Chinese blue-and- white porcelain, Ming dynasty, Kraak porcelain

1 Introduction

Porcelain belongs to the group of earthenwares and ceramics, but distinguishes itself through properties like hardness, whiteness and non-porosity. The body of this ceramic is made of porcelain stone and China clay or kaolin. [1] Subsequently a decorative pigment layer can be added together with a protecting, impervious layer of glaze. [2] In case blue and white pigments are present under the glaze, defining a characteristic blue/white appearance, the ceramic is called Chinese blue-and-white porcelain. The production and use of this kind of porcelain flourished in the Yuan dynasty (1271 - 1368) and the Ming dynasty (1368 - 1644) in China. Objects made of blue-and-white porcelain were considered precious and valuable pieces of art and were consequently desired by many

emperors of China. Jingdezhen was the largest manufacturing center, where folk and imperial kilns (porcelain production places) were located. Folk kilns were known to produce export wares and the imperial kilns supplied the royal court with fine porcelain ceramic. [2] [3] [4] Everything in the imperial kiln, from raw material to end product, was strictly regulated and submitted to sharp criteria in order to guarantee quality standards, furthermore it was possible that products and materials had to change due to a shift in regime, resulting in another porcelain elemental fingerprint. [5] Until now, the dating procedure of archaeological porcelain samples, was mainly performed via an art-historical approach, differentiating based on the specific styles of porcelain originating from different eras throughout the Chinese history. [6] The stylistic attributes considered are mainly influenced by the different likes and dislikes of the various emperors in power. However, this method could fail in some cases, for instance when counterfeit pieces are encountered and consequently a more accurate dating procedure is desirable. The method utilized in this article is based on the use of quantitative X-ray fluorescence (XRF) spectroscopic measurements and the determination of (trace) elemental distributions and fingerprints within the different regions of interest of the porcelain fragments, being the clay body and the pigment and glaze layer. [7] This approach is possible due to variations in the elemental fingerprints, originating from the use of different (raw) materials chosen by the empire, present in the porcelain fragments. The oldest findings of Chinese porcelain date back to the Han dynasty, between 206 BC and 220 AD [8], thereby contributing to more than 2000 years of porcelain history and rendering the dating process not so straightforward without reference material, both in time and space. Therefore two groups of kraak porcelain samples are examined using X-ray (micro) spectroscopic and chemometric methods: one group has been submerged in the ocean for 4 centuries and the other group is represented by a sample which has been stored in a dry environment, which gives the opportunity to observe the potential impact of environmental factors on the results. [9] Previous XRF spectroscopy work on porcelain and earthenware was performed for provenance determination [10] [11], for conservation studies[12] and to determine the elemental composition in the different porcelain layers[13] [14], i.e. body, pigment and glaze, which can also be determined for instance by SEM[14] or PIXE[15] [16] experiments. To obtain additional information on the used pigment, next to the elemental composition[5], cobalt K-edge X-ray absorption near edge structure (XANES) measurements were performed.[17]

2 Materials and Methods

2.1 Samples

Two groups of blue and white porcelain samples were investigated using X-ray fluorescence (XRF) spectroscopy; the first group (A, Fig. 1 left) consists of ten shards discovered close to the Malaysian coast in 1997 and retrieved by a team of underwater archaeologists from a Portuguese shipwreck in 2003 [18]. The second group (B, Fig. 1 right) consists of a shard from a plate belonging to a private collection. Via art-historical

analyses, both groups were determined as kraak porcelain (i.e. porcelain destined for trade to Europe) originating from the Ming dynasty (1368 - 1644). It is thought that the word kraak comes from the Dutch word for the Portuguese merchant ships or carracks. [6]



Figure 1: Left: 10 porcelain shards from group A, front and back. Right: porcelain plate from group B, before and after cleaning

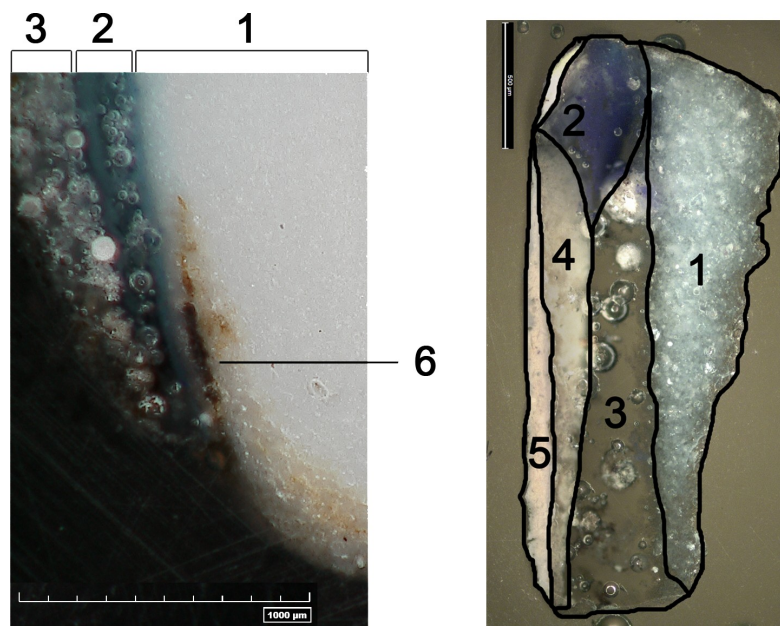


Figure 2: Left: optical image of the cross section of sample 10 from group A, indicating (1) porcelain body, (2) underglaze pigment layer, (3) glaze layer, (6) iron contamination. Right: cross section from the sample from group B, indicating (1) porcelain body, (2) pigment layer, (3) transparent glaze, (4) white glaze, (5) white unknown layer

In Fig. 2 the cross section of sample 10 (group A) and the cross section of the porcelain fragment, illustrating group B, are displayed. The porcelain shards from group A were sectioned with a diamond saw and the investigated piece for group B was sampled while removing the glue for cleaning and conservation. The samples were embedded in a Stuers resin containing 25 parts per volume of *EpoFix*[®] resin and 3 parts per volume of *EpoFix*[®] hardener. Subsequently, the samples were dried for at least 24 hours and polished by a *LaboPol-5*[®] instrument (Stuers) using P220, P500, P1200, P2400 and P4000 sandpaper and by hand using P2400, P3600, P4000, P6000, P8000 and P12000 sandpaper (listed from coarse to fine).



Figure 3: A: Cutting a porcelain shard with a diamond saw. B: Sample in a tripod for stability. C: Placement of the tripod in the cup. D: Filling the cup with the epoxy mixture.

2.2 Laboratory micro-XRF spectroscopy

Laboratory non-destructive μ -XRF measurements were performed using an EDAX Eagle-III, (EDAX, Inc., Mahwah, NJ, USA) scanning μ -XRF spectrometer. This device is equipped with a rhodium X-ray tube and a liquid N₂ cooled energy dispersive Si(Li)-detector, with an active detector area of 80 mm². It functions at a maximum efficiency with a 40 kV tube voltage and a tube current which corresponds with a 30% dead time. The X-rays penetrate the sample under an incidence angle of 65°, the beam size is defined by a polycapillary optic (X-ray Optical Systems, Inc., NY, USA) and can reach values between 25 μ m and 315 μ m. Two microscope magnifications (10x and 100x) are used to align the sample in the focal spot of the beam. All measurements were performed with a 25 μ m beam and in a vacuum environment, which allows the detection of low atomic number elements (down to Na), since the corresponding low energetic XRF-lines are not attenuated by air. Quantification was performed through a fundamental parameter based standardless method, as implemented in the EDAX Eagle III software package. Afterwards the data was processed using the AXIL [19] and *Microxrf2* software packages. All experiments were performed on porcelain cross sections to avoid detecting signal from different layers simultaneously, due to the penetration depth of the incident X-ray photons.

2.3 Synchrotron X-ray absorption spectroscopy

Microbeam X-ray absorption near edge structure (XANES) measurements were performed at the Dutch-Belgian Beamline (DUBBLE- BM26A) at the European Synchrotron Radiation Facility (ESRF) in Grenoble, France. The X-rays at BM26A are originating from a 0.4 T bending magnet source. The beam has an approximate photon flux of 1×10^9 photons/s, after focusing the primary beam with a polycapillary optic (X-ray Optical Systems, Inc., NY, USA) to a 0.5 μ m (H) x 1 μ m (V) beam. The energy is selected by a Si(111) monochromator, with an energy resolution of $\Delta E/E = 2 \times 10^{-4}$. The incoming flux and the flux after transmission through the sample are measured by ionization chambers for transmission mode. In case of fluorescence mode, the sample is positioned under an angle of 45° with respect to the incoming beam and the emerging fluorescence is detected with a Radiant Vortex-EM silicon drift detector (SDD), which is positioned at 90° relative to the incoming beam. In order to reduce scattering from the sample environment reaching the detector an aluminum collimator is added to the detector. XANES measurements were performed on the Co edge ($E_0 = 7.709$ keV) with a scan range of -100 eV to +150 eV with respect to E_0 . The reference compounds were measured in transmission mode whereas the samples were measured in fluorescence mode.

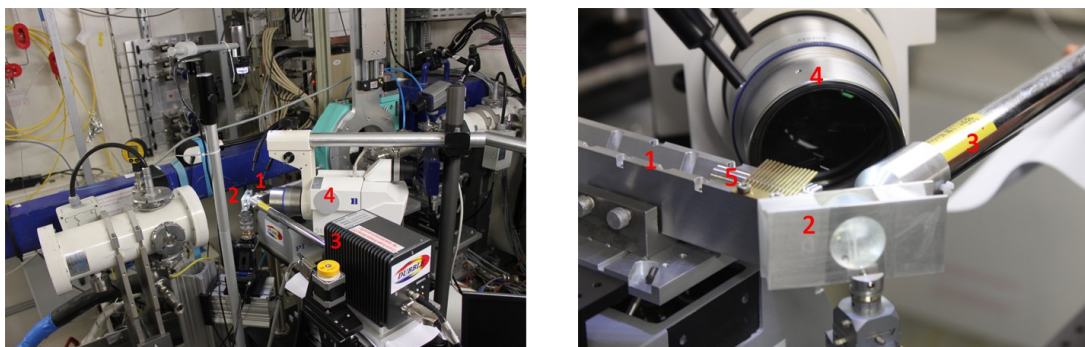


Figure 4: Dubble setup left: overview of the setup at the DUBBLE beamline. Right: zoomed image on the sample with 1: Incoming beam direction with a polycapillary optic 2: Porcelain sample mounted between aluminium brackets 3: Vortex EM SDD detector 4: microscope 5: polycapillary optic

3 Results and Discussion

Fig. 5 and Fig. 6 show elemental maps acquired by micro-XRF scans on respectively group A (sample 10) and group B using an EDAX Eagle-III spectrometer. Both groups have a *Si* and *K* distribution over the entire porcelain cross section, the body and glaze are defined by *Al* and *Ca* respectively and the underglaze pigment is characterized by the presence of *Co* and *Ni*. In group A an iron hotspot is visible in the porcelain body, which could indicate to a contamination in the used raw materials. The sample analyzed for group B has an extra white layer on top of the glaze layer, characterized by the presence of *S*, *Ti*, *Cu* and *Zn*. This layer could be identified as a white paint layer, added to the porcelain during a previous conservation attempt. Since *TiO₂* and *ZnO* were used instead of *PbO₂* as a pigment in the paint, it is safe to assume the layer was most likely added after 1920. [20]

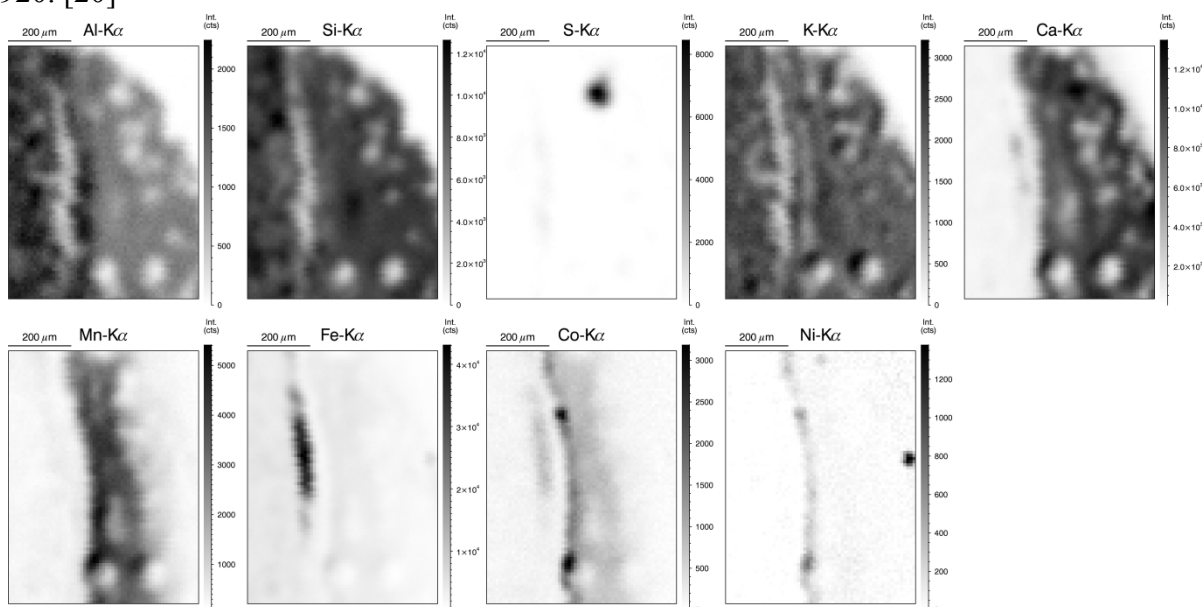


Figure 5: Micro-XRF spectroscopy elemental cross sectional images for group A, elemental distribution shown for sample 10. Most relevant elements are shown, other elements measured are: *Mg*, *Cl*, *Ti*, *Cu*, *Zn*, *Ga*, *Rb*, *Sr*, *Mo*, *Rh*, *Ba* and *Ce*. *Rh* L lines originate from the rhodium X-ray source.

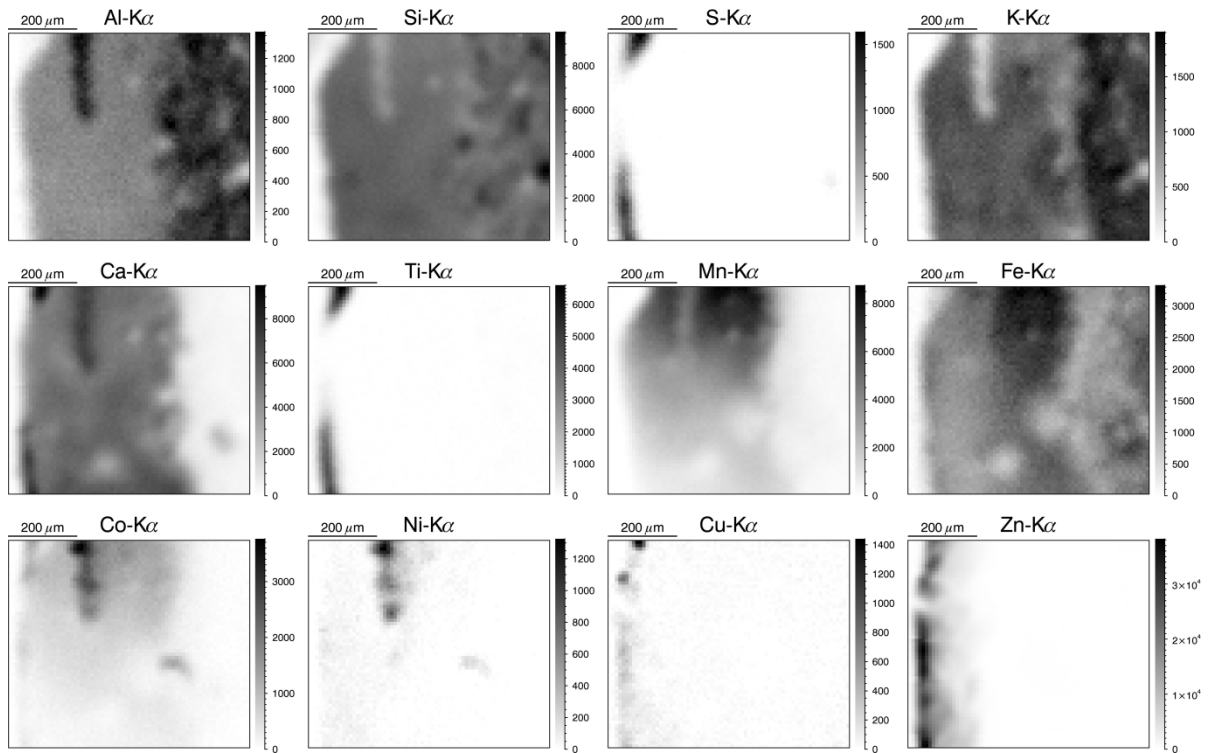


Figure 6: Micro-XRF spectroscopy elemental cross sectional images for group B. Most relevant elements are shown, other elements measured are: Mg, Cl, Ga, Rb, Sr, Mo, Rh, Ba and Ce. Rh – L lines originate from the rhodium X-ray source.

Quantified results from the EDAX Eagle-III are represented for group A in table 1, 2 and 3 for respectively the body, the glaze and the pigment and for group B in table 4 for the body, transparent glaze, the white glaze, the pigment and the white paint layers. The elements listed in the table are those used in further analysis.

Sample	Al ₂ O ₃	SiO ₂	K ₂ O	CaO	TiO ₂	MnO	Fe ₂ O ₃	CoO
1	21.43 (2.90)	69.08 (3.99)	4.02 (0.40)	0.72 (0.39)	0.08 (0.01)	0.08 (0.02)	1.21 (0.22)	0.06 (0.01)
2	22.79 (1.10)	68.99 (1.04)	4.31 (0.06)	1.20 (0.05)	0.08 (0.04)	0.08 (0.01)	1.05 (0.13)	0.05 (0.01)
3	20.90 (3.40)	71.21 (3.45)	4.02 (0.10)	1.24 (0.20)	0.11 (0.04)	0.08 (0.02)	1.02 (0.20)	0.04 (0.01)
4	23.64 (1.01)	66.70 (1.81)	5.01 (0.34)	1.67 (0.23)	0.12 (0.04)	0.07 (0.00)	1.40 (0.09)	0.05 (0.01)
5	22.12 (1.76)	69.34 (2.16)	4.25 (0.20)	1.12 (0.38)	0.10 (0.04)	0.09 (0.01)	1.38 (0.12)	0.05 (0.00)
6	20.85 (1.69)	70.45 (1.71)	3.07 (0.23)	0.69 (0.10)	0.04 (0.01)	0.37 (0.42)	0.59 (0.46)	0.03 (0.03)
7	20.20 (0.78)	66.72 (2.82)	3.66 (0.61)	3.59 (4.68)	0.07 (0.02)	0.06 (0.01)	1.05 (0.21)	0.05 (0.01)
8	21.79 (2.44)	68.54 (2.48)	4.39 (0.07)	0.86 (0.33)	0.08 (0.01)	0.09 (0.02)	1.37 (0.18)	0.07 (0.00)
9	23.87 (1.84)	66.34 (1.96)	4.49 (0.06)	0.50 (0.12)	0.07 (0.01)	0.11 (0.01)	1.57 (0.07)	0.11 (0.01)
10	21.45 (1.61)	69.37 (1.87)	4.42 (0.29)	1.01 (0.34)	0.06 (0.02)	0.10 (0.02)	1.38 (0.15)	0.08 (0.01)

Table 1: Calculated oxide concentrations (wt%) in the body for group A, including the standard deviation on the measurements between brackets.

Sample	Al ₂ O ₃	SiO ₂	K ₂ O	CaO	TiO ₂	MnO	Fe ₂ O ₃	CoO
1	14.09 (0.38)	69.98 (1.09)	4.56 (0.21)	6.16 (0.46)	0.06 (0.01)	0.11 (0.01)	1.38 (0.12)	0.06 (0.01)
2	14.66 (1.26)	68.42 (1.15)	3.74 (0.23)	10.39 (1.09)	0.06 (0.01)	0.12 (0.01)	1.07 (0.09)	0.05 (0.00)
3	13.66 (0.56)	68.73 (0.75)	3.32 (0.46)	11.22 (1.54)	0.08 (0.01)	0.10 (0.01)	1.04 (0.11)	0.04 (0.00)
4	12.63 (1.73)	69.31 (3.18)	3.78 (0.33)	11.92 (1.59)	0.07 (0.01)	0.10 (0.00)	1.13 (0.10)	0.04 (0.00)
5	14.77 (4.36)	68.89 (2.95)	3.67 (0.46)	9.87 (0.77)	0.08 (0.02)	0.09 (0.03)	1.02 (0.27)	0.03 (0.01)
6	15.97 (2.06)	69.40 (2.19)	3.20 (0.30)	5.82 (1.25)	0.07 (0.01)	0.56 (0.08)	1.03 (0.09)	0.21 (0.03)
7	13.70 (1.79)	66.55 (1.03)	3.50 (0.32)	10.60 (0.93)	0.06 (0.00)	0.12 (0.02)	1.12 (0.23)	0.05 (0.01)
8	11.03 (1.23)	58.22 (4.81)	4.56 (0.64)	17.45 (2.22)	0.10 (0.02)	0.23 (0.06)	3.07 (1.12)	0.13 (0.05)
9	12.41 (3.00)	55.70 (14.41)	5.20 (1.25)	17.28 (8.05)	0.09 (0.07)	0.27 (0.24)	2.66 (2.59)	0.18 (0.16)
10	11.60 (0.21)	66.36 (2.05)	3.55 (0.13)	15.30 (2.11)	0.05 (0.01)	0.09 (0.03)	0.90 (0.36)	0.05 (0.02)

Table 2: Calculated oxide concentrations (wt%) in the glaze layer for group A, including the standard deviation on the measurements between brackets.

Sample	Al ₂ O ₃	SiO ₂	K ₂ O	CaO	TiO ₂	MnO	Fe ₂ O ₃	CoO	Ni ₂ O ₃
1	19.68 (2.46)	64.60 (3.79)	4.20 (0.06)	5.96 (4.65)	0.07 (0.02)	1.42 (0.80)	1.15 (0.42)	0.56 (0.43)	0.04 (0.05)
2	19.89 (0.60)	63.58 (7.02)	2.95 (1.32)	8.04 (5.86)	0.08 (0.01)	1.74 (1.39)	1.12 (0.42)	0.58 (0.50)	0.14 (0.15)
3	18.96 (1.95)	58.00 (2.01)	2.10 (0.39)	12.51 (0.32)	0.12 (0.02)	3.05 (0.25)	1.88 (0.21)	1.41 (0.18)	0.22 (0.08)
4	18.79 (0.69)	59.66 (1.17)	2.98 (0.13)	10.92 (1.41)	0.09 (0.04)	1.79 (0.83)	1.63 (0.42)	0.83 (0.45)	0.24 (0.16)
5	21.40 (1.77)	54.58 (3.98)	1.98 (0.35)	11.50 (1.49)	0.06 (0.02)	2.40 (0.64)	1.32 (0.24)	1.14 (0.47)	0.22 (0.08)
6	15.07 (2.81)	70.82 (3.86)	3.09 (0.42)	5.47 (1.94)	0.05 (0.01)	0.73 (0.10)	1.04 (0.11)	0.31 (0.05)	0.02 (0.01)
7	17.07 (1.44)	58.78 (2.27)	2.18 (0.43)	12.47 (1.27)	0.08 (0.03)	2.97 (0.24)	1.76 (0.20)	0.78 (0.20)	0.31 (0.22)
8	13.60 (2.98)	59.35 (2.61)	3.27 (1.38)	13.90 (1.30)	0.09 (0.03)	2.41 (0.26)	2.76 (1.38)	0.82 (0.25)	0.20 (0.03)
9	19.50 (0.97)	58.18 (2.33)	2.26 (0.39)	10.69 (0.89)	0.08 (0.01)	3.10 (0.94)	1.81 (0.35)	1.24 (0.49)	0.18 (0.06)
10	14.97 (0.89)	62.55 (1.94)	3.10 (0.18)	11.96 (0.31)	0.08 (0.02)	1.45 (0.22)	1.65 (0.06)	0.44 (0.06)	0.08 (0.02)

Table 3: Calculated oxide concentrations (wt%) in the pigment layer for group A, including the standard deviation on the measurements between brackets.

Oxide	Body	Tr. Glaze	W. Glaze	Oxide	Pigment	W. Paint
Al ₂ O ₃	22.95 (0.34)	12.46 (0.54)	10.98 (0.98)	Al ₂ O ₃	14.44 (1.75)	4.31 (2.41)
SiO ₂	68.37 (0.35)	65.08 (0.78)	69.02 (2.79)	SiO ₂	59.94 (1.58)	23.55 (18.30)
K ₂ O	3.90 (0.08)	3.81 (0.42)	6.97 (6.29)	K ₂ O	2.23 (0.39)	0.98 (0.76)
CaO	0.52 (0.06)	14.57 (0.70)	8.64 (7.62)	CaO	13.01 (0.58)	24.20 (10.48)
TiO ₂	0.05 (0.01)	0.06 (0.01)	0.16 (0.17)	TiO ₂	0.05 (0.02)	9.12 (4.20)
MnO	0.07 (0.01)	0.73 (0.33)	0.68 (0.06)	MnO	4.39 (0.47)	0.04 (0.04)
Fe ₂ O ₃	1.02 (0.12)	1.19 (0.12)	0.49 (0.38)	Fe ₂ O ₃	1.74 (0.14)	1.37 (0.52)
CoO	0.06 (0.01)	0.11 (0.04)	0.06 (0.04)	CoO	1.00 (0.00)	0.05 (0.00)
ZnO	0.09 (0.06)	0.02 (0.00)	0.29 (0.08)	Ni ₂ O ₃	0.24 (0.04)	0.03 (0.02)
				ZnO	0.18 (0.14)	6.61 (3.19)

Table 4: Calculated oxide concentrations (wt%) in the body, the transparent glaze layer, the white glaze layer, the pigment layer and in the paint layer for group B, including the standard deviation on the measurements between brackets.

The statistical evaluation of the quantified results was performed using the data analysis software IBM SPSS® version 23. Groups A en B were compared in terms of oxide concentrations in the various regions of interest. [21] The oxides selected for the principal component analysis or PCA [22] on the body were Al₂O₃, SiO₂, K₂O and TiO₂, which are chosen for their constant oxide concentrations through the porcelain. Since Al₂O₃ is also present in the pigment layer, it was exchanged for CaO during the analysis of the glaze and pigment layers.

The outcome of the PCA analysis is shown in the score plot, Fig. 7, where it can be seen that the data originating from group A is distributed closely around the points corresponding to group B, which means that both groups have similar elemental composition and were therefore made with similar raw materials. Together with the art-historical analysis this indicated that both groups of porcelain were manufactured in the same time period and in the same or a nearby located kiln. The distribution of the data points corresponding to the body is more centered around the reference value (obtained

from B) compared to the points of the glaze and pigment, this could indicate that the raw materials used for the body were all located in the same region or mining field, while the material for the pigment and the glaze could come from more diverse regions. Subsequently it can be observed that the white paint layer from group B is clearly different compared to the other data points.

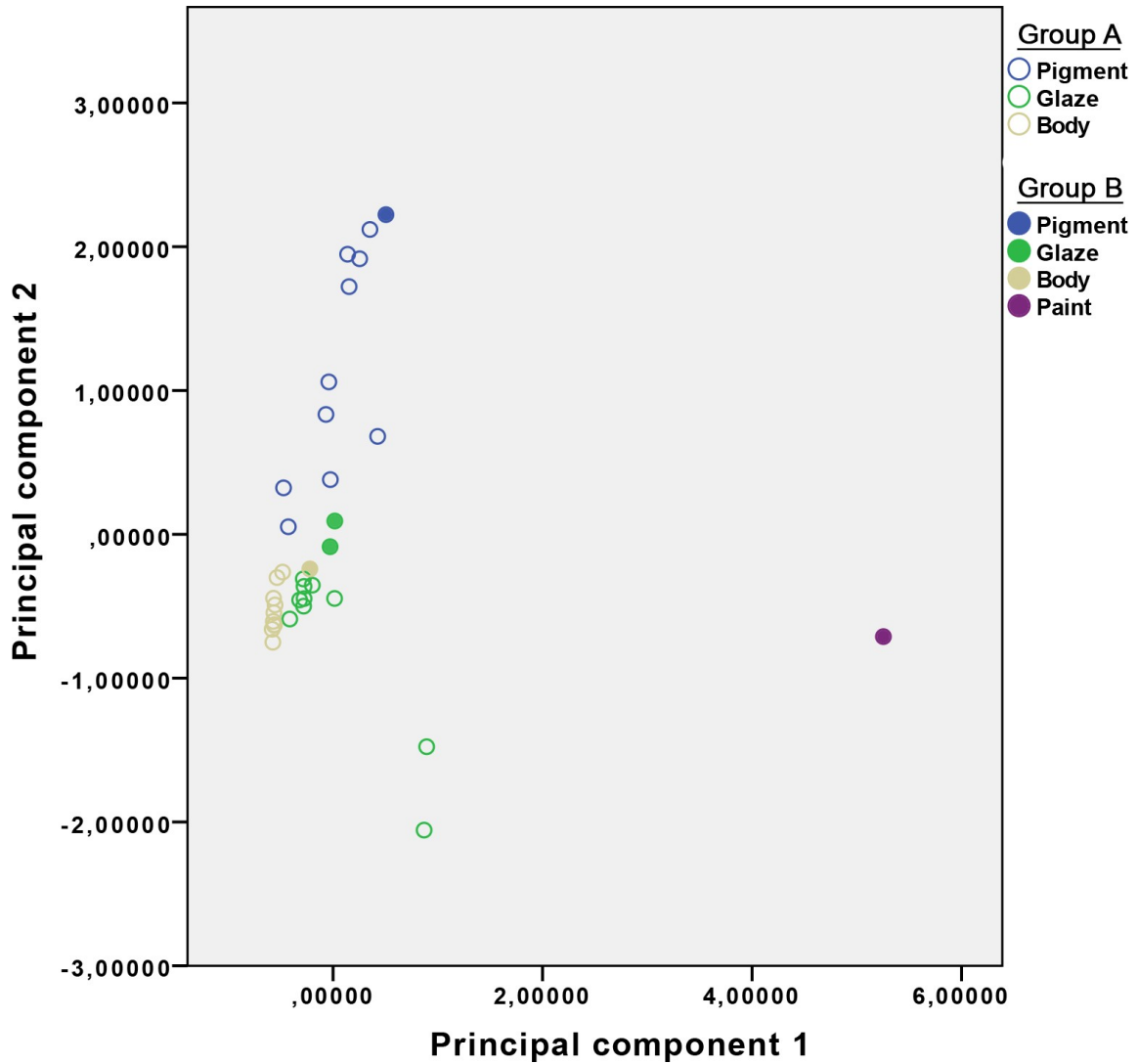


Figure 7: PCA score plot SPSS® output for both groups and the entire porcelain cross section divided in the specific regions of interest. Group A and B have both the body, glaze and pigment, where group B also has the paint layer and twice the glaze region of interest due to the transparent glaze and the white glaze layer.

Initial information regarding the blue pigment has been obtained with the XRF spectroscopic mappings, demonstrated for cobalt in Fig. 8 for sample 2 (group A), where the curled feature in the blue region is clearly observed in the mapping. Cobalt is the characteristic element in the frequently used imported or local cobalt-blue underglaze pigment for light and dark blue paintings on the porcelain body.[5] [15] [23] [24] [25]

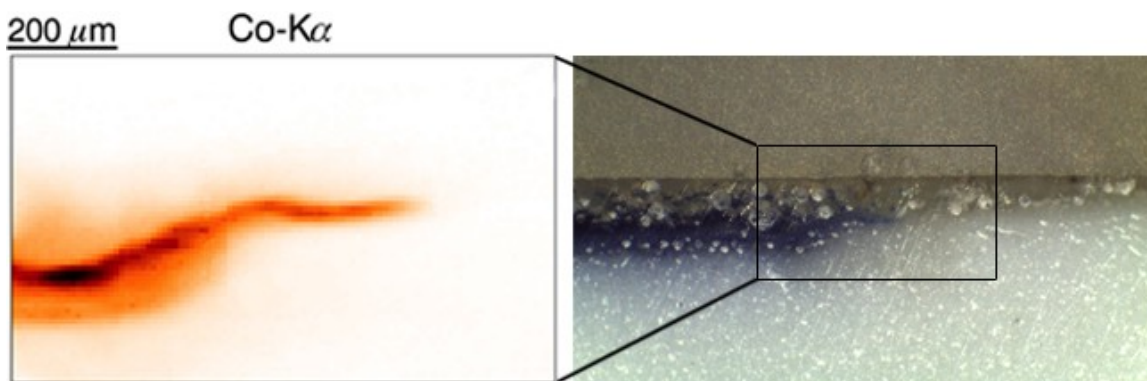


Figure 8: Comparison between the cobalt XRF spectroscopic result of sample 2 (left) and the microscopic picture of the same region (right).

To investigate the pigment further, a *Co* K-edge X-ray absorption near edge structure (XANES) measurement was taken in the pigment layer for each sample. In Fig. 9 the result for the unknown *Co*-rich layer is plotted together with the response of a measured reference sample for the Cobalt Blue pigment. The unknown blue pigment shows significant similarities with the Cobalt Blue, confirming the identity of the blue pigment used in the porcelain shards.

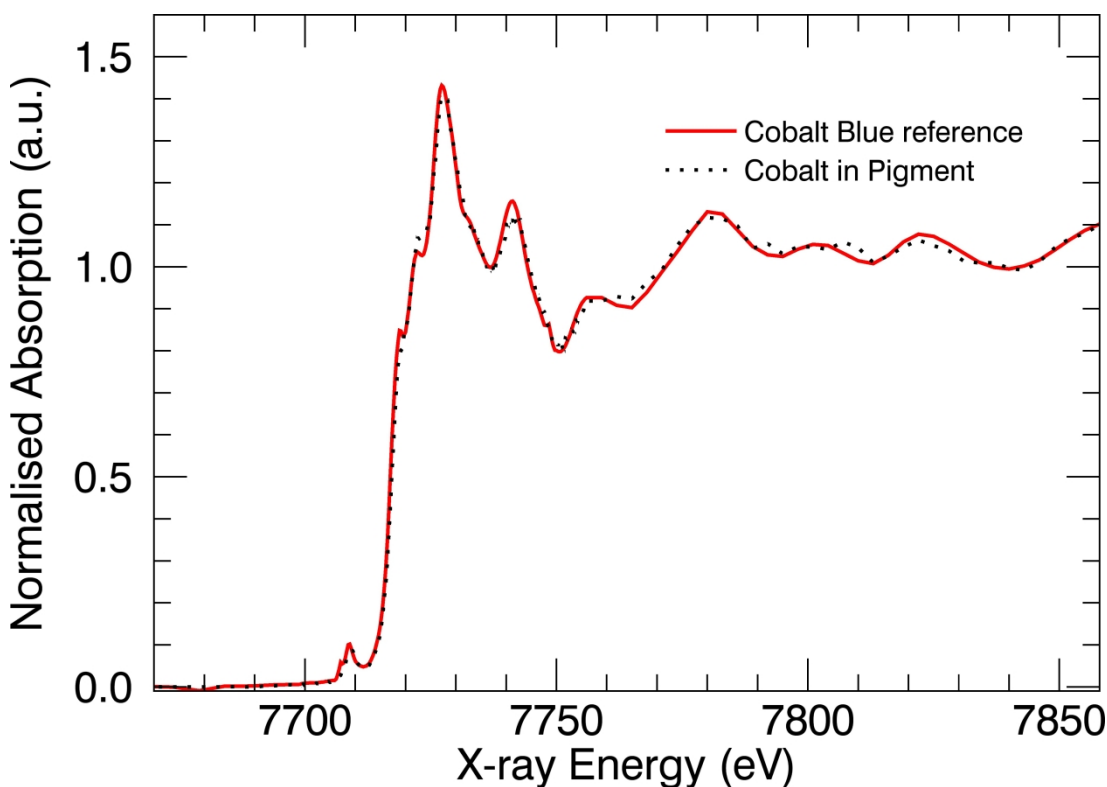


Figure 9: *Co* K-edge XANES scan of the pigment, compared to a reference of cobalt blue.

Subsequently a line scan through the porcelain cross section (range of 295 μm) was performed to examine the change of the chemical-state of *Co* across the body-pigment-glaze region, shown in Fig. 10.

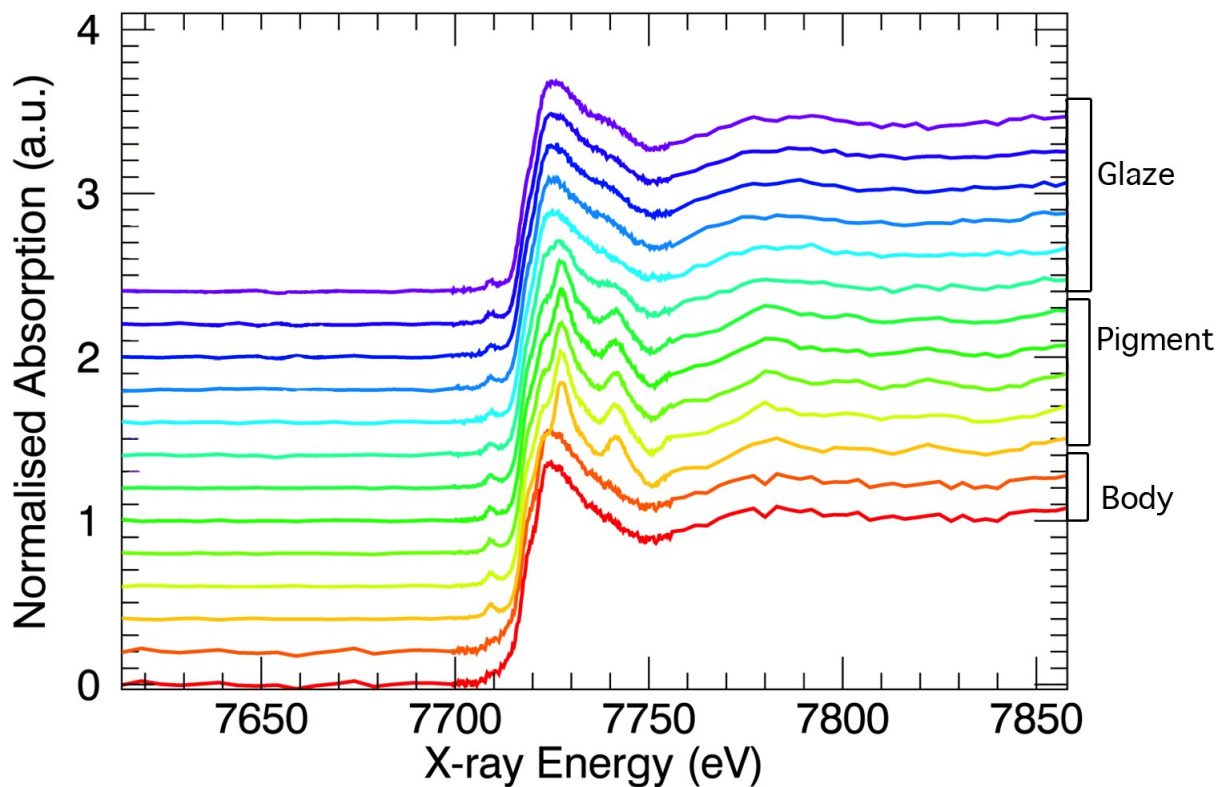


Figure 10: Cobalt K-edge XANES spectra corresponding to various locations along a straight line of 295 micron in length, across the body-pigment-glaze cross section.

Three different XANES spectra can be observed in this representation, one for the glaze, one for the pigment and one for the body. The measurements for cobalt in the glaze and the body are similar, although some differences can be noticed. The glaze still has a pre-edge peak at 7710 eV and a small increase in absorption intensity at 7740 eV, similar to the spectra of the pigment, but these features are absent in the measurements obtained from the body. The similarity between the glaze and the pigment is due to the fading of the pigment in the glaze layer before the baking process starts, therefore the glaze will contain more pure pigment compared to the body.

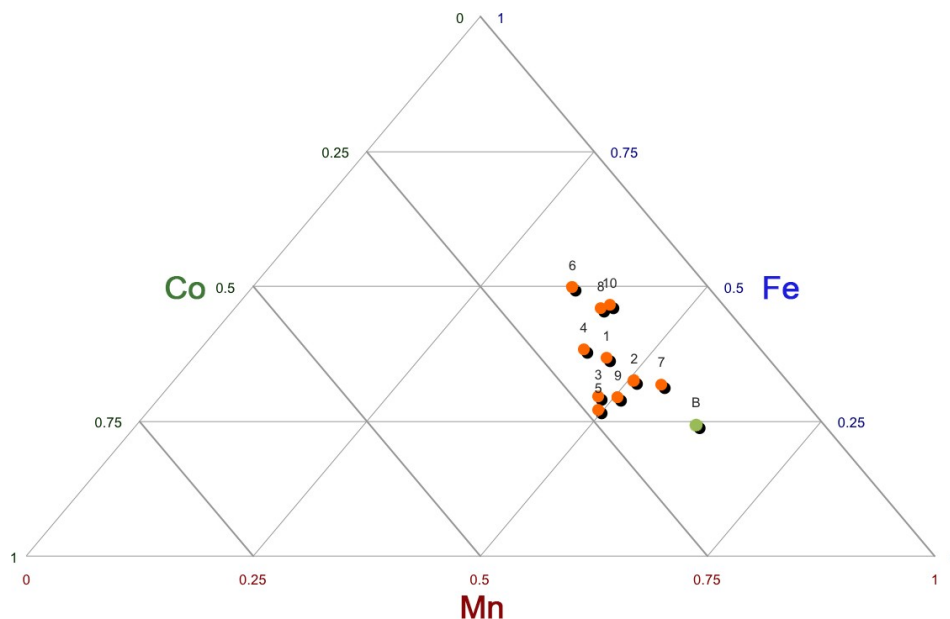


Table 5: Visual representation of the concentration of Mn, Fe and Co in a triangle diagram. Group A: orange dots, group B: green dot

In Fig. 5 the concentrations of manganese, iron and cobalt are displayed in a triangle diagram. The results are situated in the middle of the manganese concentration region and in the low cobalt and middle to high iron region. This is a close match of composition characteristics, which represents an additional indication for the common origin of group A and B.

4 Conclusion

Our results demonstrate that the two investigated groups of the Chinese blue-and-white porcelain samples exhibit similar elemental concentrations (major/minor and trace-level) fingerprints in all layers, therefore it is safe to assume that they were made of raw materials of similar origin. Group A and B have similar elemental concentrations in all layers, suggesting they were fabricated with similar raw materials. Together with the art-historical analysis this indicates that both groups of porcelain (i.e. those recovered from the sunken merchant ship and the one known to have originated from the Ming dynasty used for reference) were manufactured in the same time period and in the same or in a nearby located kiln. To differentiate if this was the imperial kiln Jingdezhen, a folk kiln nearby or one located at the coast and therefore closer to the trading routes, more comparing experiments with reference material specific for the different kilns should be performed. The body depicts comparable compositional characteristics where the glaze and pigment show a more diverse composition, this could indicate that the raw materials used for the body were all located in the same region or mining field, while the material for the pigment and the glaze could come from more diverse other regions. The white paint layer in the sample of group B is the result of an earlier conservation attempt which was performed after 1920, this could be deduced due to the use of Ti and Zn instead of Pb to make white paint. In both samples the used blue pigment is $CoAl_2O_4$, commonly

referred to as Cobalt Blue. The porcelain samples of group A were submerged 400 years in seawater, although this did not result in a difference compared to group B. This could mean that salt water has no significant influence on the elemental distribution in the porcelain.[9]

5 Acknowledgments

The authors would like to thank the staff members of DUBBLE, Dr. D. Banerjee and Dr. A. Longo for their support during the synchrotron experiments. A special thanks goes out to S. Sjostrand for providing us the samples of group A and the conservation department of the University of Antwerp for providing the porcelain sample of group B. This research was also supported by the Funds for Scientific Research Flanders (FWO) through project nr. G. 0C12.13 and G025712N.

Bibliography

1. Y. H. CT. YAP, “Raw-materials for making jingdezhen porcelain from the 5 dynasties to the qing dynasty,” *Appl Spectrosc*, 1992.
2. E. H. C. Fischer, “Export chinese blue-and-white porcelain: compositional analysis and sourcing using non-invasive portable xrf and reflectance spectroscopy,” *Journal of Archaeological Science*, vol. 80, 2017.
3. X. Feng, *Chinese ceramics*. Shanghai Classics Publishing House, 2001.
4. J. Needham, ed., *Science and civilisation in China*, vol. 5. Cambridge University Press, 2004.
5. R. Wen, C. S. Wang, Z. W. Mao, Y. Y. Huang, and A. M. Pollard, “The chemical composition of blue pigment on chinese blue-and-white porcelain of the yuan and ming dynasties (ad 1271-1644),” *Archaeometry*, vol. 49, no. 1, pp. 101–115, 2007.
6. S. G. Valenstein, *A Handbook Of Chinese Ceramics*. Metropolitan Museum of Art, 1988.
7. J. V. Pevenage, E. Verhaeven, B. Vekemans, D. Lauwers, D. Herremans, W. D. Clercq, L. Vincze, L. Moens, and P. Vandenabeele, “Illustration of compositional variations over time of chinese porcelain glazes combining micro-x-ray fluorescence spectrometry, multivariate data analysis and seger formulas,” *Spectrochimica Acta Part B: Atomic Spectroscopy*, vol. 103–104, pp. 106 – 111, 2015.
8. R. K. Temple, *The Genius of China: 3,000 Years of Science, Discovery, and Invention*. London: Andre Deutsch, 3rd edition ed., 2007.

9. Y. Chen, W. Luo, N. Li, and W. C., "A study on provenance of marine porcelains from huaguangjiao no. 1 after sample desalination," *Journal of Archaeological Science: Reports*, 2016.
10. H. Ma, J. Zhu, J. Henderson, and N. Li, "Provenance of zhangzhou export blue-and-white and its clay source," *Journal of Archaeological Science*, 2012.
11. M. Isabel Dias, M. Isabel Prudencio, M. Pinto De Matos, and A. Luisa Rodrigues, "Tracing the origin of blue and white chinese porcelain ordered for the portuguese market during the ming dynasty using inaa," *Journal of Archaeological Science*, vol. 40, pp. 3046–3057, March 2013.
12. M. Mantler and M. Schreiner, "X-ray fluorescence specrometry in art and archaeology," *X-Ray Spectrom.*, vol. 29, pp. 3–17, 2000.
13. T. Zhu, Y. Zhang, H. Xiong, Z. Feng, Q. Li, and B. Cao, "Porcelain from jingdezhen in the yuan dynasty of china (ad 1271 - 1368) by micro x-ray fluorecence spectroscopy and microscopy," *Archaeometry*, 2016.
14. P. Colombar, G. Sagon, L. Huy, N. Liem, and L. Mazerolles, "Vietnamese (15th century) blue-and-white, tam thai and lustre porcelains/stonewares: glaze composition and decoration techniques," *Archaeometry*, vol. 46, pp. 125–136, 2004.
15. H. Cheng, Z. Zhang, H. Xia, J. Jiang, and F. Yang, "Non-destructive analysis and appraisal of ancient chinese porcelain by pixe," *Nuclear Instruments and Methods in Physics Research B*, vol. 190, pp. 488–491, 2002.
16. L. V. Ferreira, D. Ferreira, D. Conceicao, L. Santos, M. Pereira, T. Casimiro, and I. F. Machado, "Portuguese tin-glazed earthenware from the 17th century. part 2: A spectroscopic characterization of pigments, glazes and pastes of the three main production centers," *Spectrochimica Acta Part A: Molecular and Biomolecular Spectroscopy*, vol. 149, pp. 285 – 294, 2015.
17. L. Wang and C. Wang, "Co speciation in blue decorations of blue-and-white porcelains from jingdezhen kiln by using xafs spectroscopy," *J. Anal. At. Spectrom.*, vol. 26, pp. 1796–1801, 2011.
18. N. M. Archaeology, "The wanli shipwreck - archaeological report." <http://www.thewanlishipwreck.com/Report.html>, 2010.
19. B. Vekemans, K. Janssens, L. Vincze, F. Adams, and P. Vanespen, "Analysis of x-ray-spectra by iterative least-squares (axil) - new developments," *X-ray Spectrometry*, vol. 23, pp. 278–285, 1994.

20. M. Laver, E.W.Fitzhugh(Ed.), *Artists' Pigments: Volume 3: A Handbook of their History and Characteristics*, National Gallery of Art (1997), Chapter 10: Titanium white, pp.295-355, 10.2307/1506685
21. J. Van Pevenage, D. Lauwers, D. Herremans, E. Verhaeven, B. Vekemans, W. De Clercq, L. Vincze, L. Moens, and P. Vandenabeele, "A combined spectroscopic study on chinese porcelain containing ruan-cai colours," *ANALYTICAL METHODS*, vol. 6, no. 2, pp. 387–394, 2014.
22. B. Vekemans, K. Janssens, L. Vincze, A. Aerts, F. Adams, and J. Hertogen, "Automated segmentation of micro-xrf image sets," *X-ray Spectrometry*, vol. 26, pp. 333–346, 1997.
23. L. M. Hurcombe, ed., *Archaeological Artefacts as Material Culture*. Routledge, 2007.
24. H. Cheng, B. Zhang, D. Zhu, F. Yang, X. Sun, and M. Guo, "Some new results of pixe study on chinese ancient porcelain," *Nuclear Instruments and Methods in Physics Research B*, pp. 527–531, 2005.
25. Y. Qu, X. Xu, X. Xi, C. Huang, and J. Yang, "Microstructure characteristics of blue-and-white porcelain from the folk kiln of ming and qing dynasties," *Ceramics International*, vol. 40, pp. 8783–8790, 2014.